http://dx.doi.org/10.5012/bkcs.2014.35.3.721

Dissociation of the Pyridazine Molecular Ion†

Min Kyoung Yim, Sun Hwa Jung, and Joong Chul Choe*

*Department of Chemistry, Dongguk University-Seoul, Seoul 100-715, Korea. *E-mail: jcchoe@dongguk.edu*
Received February 15, 2013, Accepted February 26, 2013

We have explored the potential energy surface for the dissociation of the pyridazine molecular ion using G3 model calculations. The pathways have been obtained for the formation of five possible $C_4H_4^{+\bullet}$ isomers by the loss of N_2 and the consecutive $H^\bullet$ loss. It is predicted that the methylenecyclopropene radical cation is the predominant product in the loss of N_2, which is formed via the allenylcarbene radical cation, and CH_2=C–C≡CH^+ is the predominant product in the consecutive $H^\bullet$ loss.

Key Words : G3//B3LYP calculation, RRKM calculation, Kinetics, Reaction pathway

Introduction

Dissociations of the benzene molecular ion and its isoelectronic species such as ionized pyridine, diazines, and triazines have been extensively studied.[1-12] Identification of the product ions is one of the most important subjects in mass spectrometry. Several techniques have been developed for this purpose, which include tandem mass spectrometry and theoretical methods. Attempts to identify the $C_4H_4^{+\bullet}$ ion formed in the dissociation of ionized benzene[2,3] or pyridine[2,6-8] have been made. An experimental study using ion cyclotron resonance mass spectrometry showed that the radical cations of methylenecyclopropene (MCP) and vinylacteylene (VA) are the main products in the loss of C_2H_2 from the benzene ion at low and high energies, respectively.[2] In a theoretical study, we proposed that these two $C_4H_4^{+\bullet}$ isomers are formed in the loss of HCN from the pyridine ion with a dramatic dependence of their branching ratio on the internal energy.[8]

In our successive studies, we attempted to theoretically identify major product ions formed in the dissociations of ionized 1,3-diazine (pyrimidine)[10] and 1,4-diazine (pyrazine).[9] The loss of HCN was the most favorable channel in both the dissociations. It was predicted that in the loss of HCN, a mixture of CH=CHC≡$NH^{+\bullet}$, CH=CHN≡$CH^{+\bullet}$, and CH_2=C=N=$CH^{+\bullet}$ is formed from the former, whereas only CH=CHNC$H^{+\bullet}$ is formed from the latter. In this work, we examined the dissociation of the pyridazine (1,2-diazine) molecular ion (**1**, Figure 1) as a final attempt to study the dissociation kinetics of ionized diazines. In the 70-eV electron ionization (EI) mass spectrum of pyridazine,[13] the peaks corresponding to $[M - N_2]^{+\bullet}$, $[M - HN_2]^+$, and $[M - 2HCN]^{+\bullet}$ are major peaks, where M denotes the molecule. The $[M - HCN]^{+\bullet}$ ion is not detected in the dissociation by EI, in contrast to the other two diazine ion isomers. In the PEPICO study by Buff and Dannacher,[14] the loss of N_2 was the only dissociation channel of **1**, and the breakdown curves for the dissociation were fitted by a Rice-Ramsperger-Kassel-Marcus (RRKM)[15] model calculation. We obtained the potential energy surfaces (PESs) for the formation of five possible $C_4H_4^{+\bullet}$ isomers by the loss of N_2 from **1** and the consecutive $H^\bullet$ loss to form $C_4H_3^+$ using quantum chemical calculations. A kinetic analysis was performed to predict the dissociation rate based on the obtained PES.

Computational Methods

The molecular orbital calculations were performed using the Gaussian 09 suite of programs.[16] The geometries of the stationary points were optimized at the unrestricted B3LYP level of the density functional theory (DFT) using the 6-31G(d) basis set. The transition state (TS) geometries that connected the stationary points were examined and checked by calculating the intrinsic reaction coordinates at the same level. For better accuracy of the energies, G3 theory calculations using the B3LYP density functional method were performed.

The RRKM expression was used to calculate the rate constants for the unimolecular reaction steps because the RRKM formula for the microcanonical ensemble was mathematically equivalent to the formula in the statistical quasi-equilibrium theory that was developed for ionic dissociations:[15]

$$k(E) = \frac{\sigma N^{\ddagger}(E-E_0)}{h\rho(E)} \quad (1)$$

In this equation, E is the internal energy of the reactant, E_0 is the critical energy of the reaction, $N^{\ddagger}$ is the sum of the TS states, ρ is the density of the reactant states, σ is the reaction path degeneracy, and h is Planck's constant. $N^{\ddagger}$ and ρ were evaluated through a direct count of the states using the Beyer-Swinehart algorithm.[17] The E_0 values for the individual steps were obtained from the G3//B3LYP calculations and were used for RRKM calculations. Each normal mode of vibration was treated as a harmonic oscillator. The vibrational frequencies that were obtained from the B3LYP/6-31G(d) calculations were scaled down by a factor of 0.9614.[18]

†This paper is to commemorate Professor Myung Soo Kim's honourable retirement.

Results and Discussion

Figure 1 shows the optimized geometries of **1** and five low-energy $C_4H_4^{+\bullet}$ ions that can be formed by the loss of N_2, the radical cations of MCP, VA, butatriene (BT), cyclobutadiene (CB), and allenylcarbene (AC). We obtained several different pathways for each formation of these five product ions, but only the lowest energy pathways will be presented. The simplest pathway for the loss of N_2 starts from the cleavage of a C–N bond to form linear isomer **2** (Figure 2). As the N_2 moiety moves far from the linear C_4H_4 backbone of **2**, the H on C5 moves to C6 to form ion-molecule complex **3**, which easily eliminates N_2 to produce $AC^{+\bullet}$. This is the lowest energy pathway in the loss of N_2 from **1**. Alternatively, **3** isomerizes to ion-molecule complex **4**, followed by dissociation to $MCP^{+\bullet}$ + N_2. The barrier for the isomerization **3** → **4** is 4 kJ mol^{-1} higher than the threshold of the dissociation **3** → $AC^{+\bullet}$ + N_2. Moreover, the TS for the former is tighter than that for the latter. Therefore, the latter is kinetically more favored than the former, and hence the formation of $AC^{+\bullet}$ is more favored than $MCP^{+\bullet}$. However, $AC^{+\bullet}$ is relatively unstable and readily isomerizes to $MCP^{+\bullet}$ with activation energy of 13 kJ mol^{-1}. For the formation of $AC^{+\bullet}$ from **1**, the internal energy of **1** should be higher than 259 kJ mol^{-1}. Then, the internal energy of $AC^{+\bullet}$ after its formation would be high enough for the isomerization to $MCP^{+\bullet}$ to occur rapidly, even though the kinetic energy release in this dissociation is considered (see Figure 2). Therefore, $AC^{+\bullet}$ is mainly formed by the loss of N_2, but it rapidly isomerizes to $MCP^{+\bullet}$. Further $H^{\bullet}$ loss from $MCP^{+\bullet}$ may occur by three pathways. The lowest-energy pathway is the formation of CH_2=C–C≡CH^+ (iso-$C_4H_3^+$) via $AC^{+\bullet}$; $MCP^{+\bullet}$ → $AC^{+\bullet}$ → iso-$C_4H_3^+$ + $H^{\bullet}$ (Figure 2). The two cyclic $C_4H_3^+$ isomers formed by the loss of $H^{\bullet}$ from the methylene group or the ring of $MCP^{+\bullet}$ are less stable than iso-$C_4H_3^+$ by 76 or

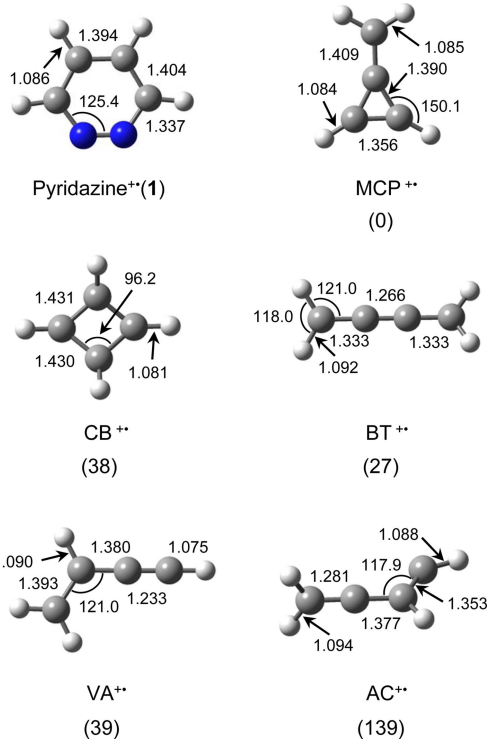

Figure 1. Geometric structures of **1** and $C_4H_4^{+\bullet}$ isomers optimized by the B3LYP/6-31G(d) calculations. The numbers are the bond lengths in Å and the angles are in degrees. The values in parentheses are relative energies of $C_4H_4^{+\bullet}$ isomers in kJ mol^{-1}, calculated by the G3//B3LYP method.

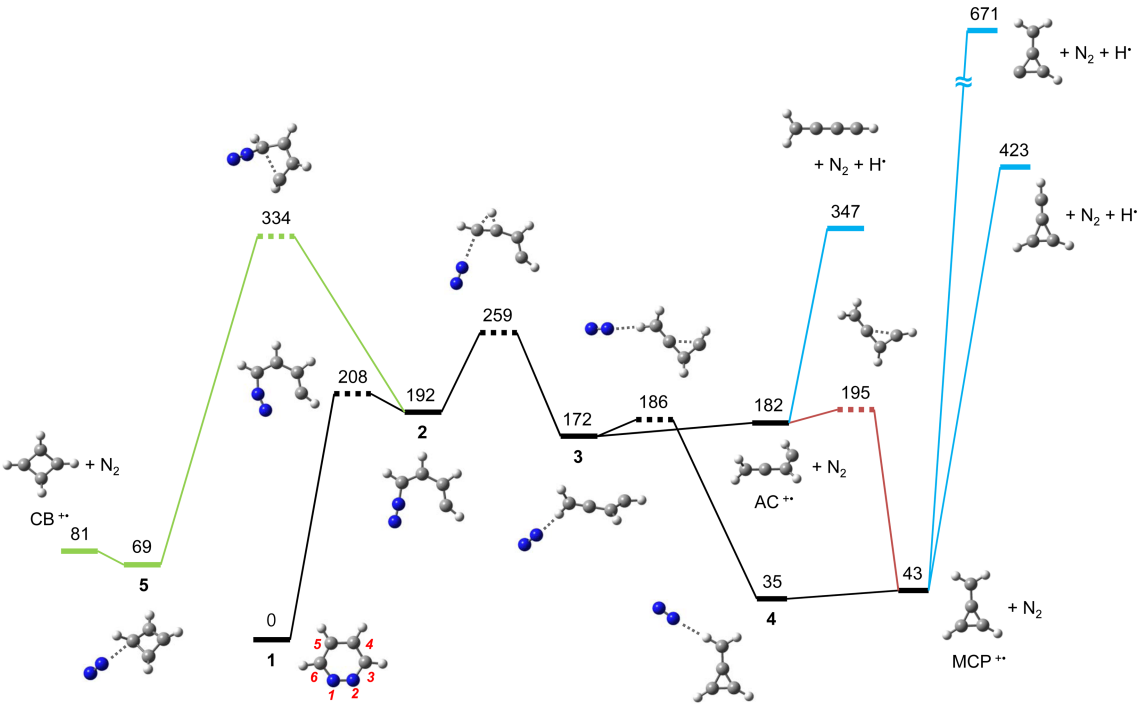

Figure 2. Potential energy diagram for the formation of $AC^{+\bullet}$, $MCP^{+\bullet}$, and $CB^{+\bullet}$ by the loss of HCN from **1**, and the consecutive H loss, derived from the G3//B3LYP calculations. The energies are presented in kJ mol^{-1}.

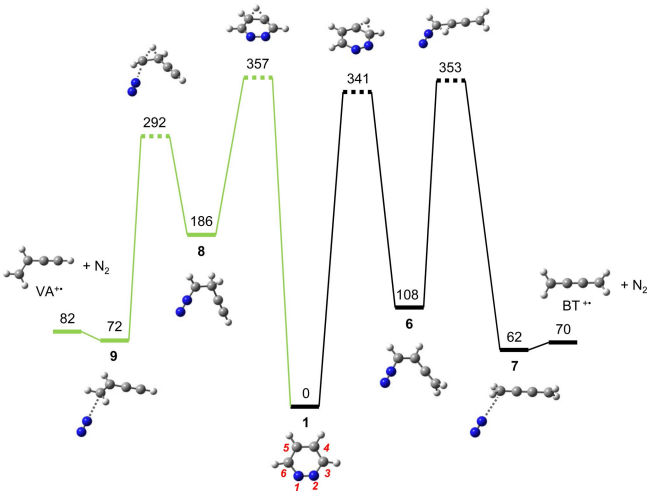

Figure 3. Potential energy diagram for the formation of $BT^{+\bullet}$ and $VA^{+\bullet}$ by the loss of HCN from **1**, derived from the G3//B3LYP calculations. The energies are presented in kJ mol^{-1}.

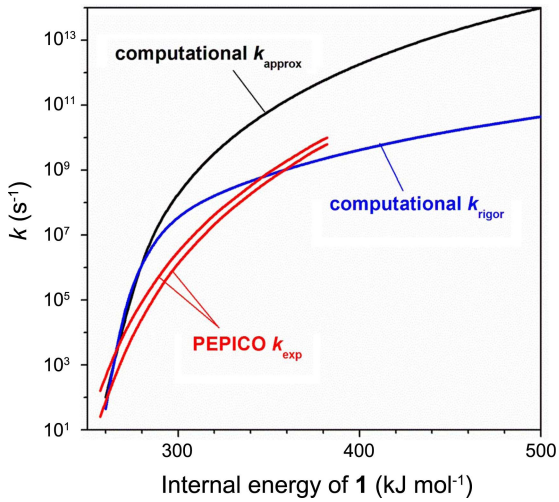

Figure 4. Theoretical and experimental energy dependences of the rate constant for the loss of HCN from **1**. The PEPICO data by Buff and Dannacher[14] were obtained so that the experimental breakdown curves measured at ion source residence times of 1 and 6 ms achieved best fits by calculations that used the RRKM $k_{exp}(E)$ curves. The results are presented as the lower and upper lines, respectively. $k_{approx}(E)$ is the RRKM result calculated by assuming that the loss of HCN occurs to form $MCP^{+\bullet}$ by one step. $k_{rigor}(E)$ is the theoretical result calculated with considering all the steps to form $MCP^{+\bullet}$.

324 kJ mol^{-1}, respectively.

Experimental evidence for the existence of AC has been reported,[19,20] but not for $AC^{+\bullet}$ to our knowledge. It is likely that $AC^{+\bullet}$ would hardly be observed as a stable species due to its shallow potential well as described above. However, the present result shows that $AC^{+\bullet}$ plays an important role as intermediates in the loss of N_2 and in the consecutive loss of $H^{\bullet}$.

2 may dissociate to $CB^{+\bullet} + N_2$ via ion-molecule complex **5** (Figure 2). However, the overall activation energy (334 kJ mol^{-1}) for this pathway is much higher than that (259 kJ mol^{-1}) for the formation of $MCP^{+\bullet}$. Figure 3 shows reaction pathways for the formation of the other two $C_4H_4^{+\bullet}$ isomers. As the H on C4 shifts to C3, the N2–C3 bond is cleaved to form linear isomer **6**, which dissociates to $BT^{+\bullet} + N_2$ via ion-molecule complex **7**. On the other hand, if the H on C4 shifts to C5, the N2–C3 bond is cleaved to form linear isomer **8**, which dissociates to $VA^{+\bullet} + N_2$ via ion-molecule complex **9**. However, the overall activation energies for these pathways are also much higher than that for the formation of $MCP^{+\bullet}$. $BT^{+\bullet}$ or $VA^{+\bullet}$ may lose $H^{\bullet}$ to form iso-$C_4H_3^+$, but their occurrences are not probable because they could be hardly formed in the primary dissociation of **1**.

We obtained several pathways for the loss of HCN from **1**, of which details are not presented here. The lowest-energy pathway was the formation of $CH{=}CH{=}C{=}NH^+$ but its overall activation energy (327 kJ mol^{-1}) was much higher than that of the formation of $MCP^{+\bullet} + N_2$, indicating that the loss of HCN is less favored than the loss of N_2. This agrees with the lack of detection of an $[M - HCN]^{+\bullet}$ peak in the 70-eV EI mass spectrum of pyridazine.

The PESs thus obtained suggest that the formation of $MCP^{+\bullet}$ via $AC^{+\bullet}$ is the predominant channel in the primary dissociation of **1** and the contributions of the other dissociation channels are negligible. We tried to calculate the dissociation rate constant using the RRKM formalism. One usually chooses the rate-limiting step for approximate calculation of the rate constant of a reaction occurring through several consecutive steps. Accordingly, we assumed that the dissociation to $MCP^{+\bullet} + N_2$ occurred by one step through the TS for the isomerization **2** → **3** because the barrier for passage of the TS is the highest. The energy dependence of the rate constant thus obtained, $k_{approx}(E)$, disagrees with the experimental one, $k_{exp}(E)$, as shown in Figure 4. For a rigorous estimation, all the steps in the dissociation pathway were included in the rate calculation. The detailed method has been described elsewhere.[8,21,22] Briefly, MATLAB software was used to numerically solve the coupled differential equations corresponding to the rate laws for the dissociation pathway. The rate constants for the individual steps were calculated using the RRKM formalism. The resultant $k(E)$, $k_{rigor}(E)$, is smaller than $k_{approx}(E)$ at internal energies higher than ~280 kJ mol^{-1}, and is closer to $k_{exp}(E)$, even though the agreement is not satisfactory (Figure 4). The steeper slope of $k_{approx}(E)$ than $k_{rigor}(E)$ indicates that the reaction actually undergoes passage of tighter TS than TS **2** → **3** if we assume that the reaction occurs through one step. We performed calculations of activation entropies ($\Delta S^{\ddagger}$)[15] for the important two TSs, TS **1** → **2** and TS **2** → **3**, with respect to **1**. The calculated $\Delta S^{\ddagger}$ values at 1000 K were 4.3 and 26 J mol^{-1} K^{-1}, respectively, indicating that TS **1** → **2** is tighter than TS **2** → **3**. This suggests that the first barrier (TS **1** → **2**) largely affects the dissociation rate constant even though it lies lower than the second barrier (TS **2** → **3**). This shows that the entropic factor is as important as the energetic factor in reaction kinetics.

The most probable reason for disagreement between $k_{rigor}(E)$ and $k_{exp}(E)$ is the uncertainty of TS frequencies used in RRKM calculations. The accuracy of TS frequencies obtain-

ed by quantum chemical calculations has not been evaluated. The other possibility is the accuracy of $k_{exp}(E)$. Because $k_{exp}(E)$ was estimated from the breakdown graph, more accurate experimental determinations are needed using techniques such as analysis of the PEPICO time of flight spectrum.

Conclusion

The PESs obtained theoretically for several dissociation pathways of **1** show that the loss of N_2 is the most favorable primary dissociation channel, and $MCP^{+\bullet}$, the most stable $C_4H_4^+$ isomer, is the predominant product ion. Interestingly, it is predicted that $AC^{+\bullet}$, the much less stable $C_4H_4^+$ isomer, is initially formed by the loss of N_2 and rapidly isomerizes to $MCP^{+\bullet}$. In the further loss of $H^{\bullet}$, $MCP^{+\bullet}$ mainly produces iso-$C_4H_3^+$ via $AC^{+\bullet}$. The dissociation rate constants calculated on the basis of the obtained PES are close to the previous experimental ones. Further studies are needed for better agreement between the energy dependences of theoretical and experimental rate constants.

Acknowledgments. This work was supported by the National Research Foundation of Korea Grant funded by the Korean Government (2010-0008287).

References

1. Kim, M. S.; Kwon, C. H.; Choe, J. C. *J. Chem. Phys.* **2000**, *113*, 9532.
2. Ausloos, P. *J. Am. Chem. Soc.* **1981**, *103*, 3931-3932.
3. van der Hart, W. J. *Int. J. Mass Spectrom.* **1998**, *176*, 23.
4. Klippenstein, S. J.; Faulk, J. D.; Dunbar, R. C. *J. Chem. Phys.* **1993**, *98*, 243.
5. Kühlewind, H.; Kiermeier, A.; Neusser, H. J. *J. Chem. Phys.* **1986**, *85*, 4427.
6. Lifshitz, C. *J. Phys. Chem.* **1982**, *86*, 606-612.
7. Lifshitz, C.; Gibson, D.; Levsen, K.; Dotan, I. *Int. J. Mass Spectrom. Ion Phys.* **1981**, *40*, 157-165.
8. Yim, M. K.; Choe, J. C. *J. Phys. Chem. A* **2011**, *115*, 3087-3094.
9. Jung, S. H.; Yim, M. K.; Choe, J. C. *Bull. Korean Chem. Soc.* **2011**, *32*, 2301.
10. Yim, M. K.; Jung, S. H.; Choe, J. C. *Bull. Korean Chem. Soc.* **2012**, *33*, 4098.
11. Ervasti, H. K.; Jobst, K. J.; Gerbaux, P.; Burgers, P. C.; Ruttink, P. J. A.; Terlouw, J. K. *Chem. Phys. Let.* **2009**, *482*, 211-216.
12. Porter, Q. N. *Mass Spectrometry of Heterocyclic Compounds*, 2nd ed.; John Wiley & Sons: New York, 1985.
13. *NIST Chemistry WebBook, NIST Standard Reference Database Number 69*.
14. Buff, R.; Dannacher, J. *Int. J. Mass Spectrom. Ion Processes* **1984**, *62*, 1-15.
15. Baer, T.; Hase, W. L. *Unimolecular Reaction Dynamics: Theory and Experiments*; Oxford University Press: New York, 1996.
16. Frisch, M. J. T., G. W.; Schlegel, H. B.; Scuseria, G. E.; Robb, M. A.; Cheeseman, J. R.; Scalmani, G.; Barone, V.; Mennucci, B.; Petersson, G. A.; Nakatsuji, H.; Caricato, M.; Li, X.; Hratchian, H. P.; Izmaylov, A. F.; Bloino, J.; Zheng, G.; Sonnenberg, J. L.; Hada, M.; Ehara, M.; Toyota, K.; Fukuda, R.; Hasegawa, J.; Ishida, M.; Nakajima, T.; Honda, Y.; Kitao, O.; Nakai, H.; Vreven, T.; Montgomery, J. A., Jr.; Peralta, J. E.; Ogliaro, F.; Bearpark, M.; Heyd, J. J.; Brothers, E.; Kudin, K. N.; Staroverov, V. N.; Kobayashi, R.; Normand, J.; Raghavachari, K.; Rendell, A.; Burant, J. C.; Iyengar, S. S.; Tomasi, J.; Cossi, M.; Rega, N.; Millam, N. J.; Klene, M.; Knox, J. E.; Cross, J. B.; Bakken, V.; Adamo, C.; Jaramillo, J.; Gomperts, R.; Stratmann, R. E.; Yazyev, O.; Austin, A. J.; Cammi, R.; Pomelli, C.; Ochterski, J. W.; Martin, R. L.; Morokuma, K.; Zakrzewski, V. G.; Voth, G. A.; Salvador, P.; Dannenberg, J. J.; Dapprich, S.; Daniels, A. D.; Farkas, Ö.; Foresman, J. B.; Ortiz, J. V.; Cioslowski, J.; Fox, D. J. *Gaussian 09, revision A. 02*; Gaussian, Inc., Wallingford CT, 2009.
17. Beyer, T.; Swinehart, D. R. *ACM Commun.* **1973**, *16*, 379.
18. Scott, A. P.; Radom, L. *J. Phys. Chem. A* **1996**, *100*, 16502.
19. Wrobel, R.; Sander, W.; Cremer, D.; Kraka, E. *J. Phys. Chem. A* **2000**, *104*, 3819-3825.
20. Aycard, J. P.; Allouche, A.; Cossu, M.; Hillebrand, M. *J. Phys. Chem. A* **1999**, *103*, 9013-9021.
21. Kim, S. Y.; Choe, J. C. *Int. J. Mass Spectrom.* **2010**, *294*, 40-46.
22. Kim, S. Y.; Choe, J. C. *Int. J. Mass Spectrom.* **2010**, *295*, 65-71.